Science Advances
AAAS
Manuscript Template

The gathering firestorm in southern Amazonia

Authors
P.M. Brando[1,2,*], B. Soares-Filho[3], L. Rodrigues[3], A. Assunção[3], D. Morton[4], D. Tuchschneider[5], E. C. M. Fernandes[5], M.N. Macedo[1,2], U Oliveira[3], M.T. Coe[1,2]

Affiliations
[1]Woods Hole Research Center, 149 Woods Hole Rd, Falmouth, MA, 02540, USA.
[2]Instituto de Pesquisa Ambiental da Amazônia (IPAM), SHIN, CA-5, Brasilia, DF, 7500, Brazil.
[3] Centro de Sensoriamento Remoto, Instituto de Geociências, Universidade Federal de Minas Gerais – UFMG, Av. Antonio Carlos 6627, CEP 31270-901, Belo Horizonte, MG, Brazil
[4]NASA Goddard Space Flight Center, Greenbelt, MD 20771, USA
[5]Agriculture Global Practice, World Bank, 1818 H. St. NW, Washington DC, 20433, USA

Abstract

Wildfires threaten to revert the capacity of Amazon forests to store carbon, spurred by interactions between extreme weather events and land-use change. Here, we develop and apply a coupled ecosystem-fire model to quantify how committed regional drying and warming for the southern Brazilian Amazon would affect wildfires and associated CO_2 emissions. Our results indicate that projected climatic changes for the region will double the area burned by wildfires, affecting up to 16% of the region's forests by 2050. Although these fires could emit as much as 17.0 Pg of CO_2 equivalent to the atmosphere, avoiding new deforestation could cut burned area and total net fire emissions in half and help prevent fires from escaping into protected areas and indigenous lands. Amazon fire regimes are projected to intensify under both low- and high-emission climate scenarios, underscoring the need for novel mitigation measures. Aggressive regional efforts to eliminate ignition sources and suppress wildfires will be critical to conserve southern Amazon forests.

MAIN TEXT

Introduction

Greenhouse gas emissions (*GHG*) accumulating in the atmosphere may push Amazon forests into a new low-biomass state by altering regional precipitation and temperature regimes. This climate-induced forest transition could release large amounts of *GHGs* to the atmosphere and accelerate global warming (*1*). Although CO_2 fertilization of forests may partially offset the projected climate-induced forest dieback (*2*), most models addressing this issue lack representation of important negative processes, including wildfires (*3*). Fire disturbance is already driving large-scale forest mortality across the drier portions of the Amazon Basin (*4*) and is likely to expand into wetter areas as climate and land use change (*5*). Ignoring this potentially large source of *GHG* emissions to the atmosphere may restrict our ability to effectively mitigate climate change, and, as a result, to conserve Amazon forests. A better understanding of future fire regimes in Amazonia could guide efforts to increase regional capacity to prevent accidental forest fires and their negative impacts on ecosystem services, socioeconomic well-being, and biodiversity (*6*).

Deforestation in the Brazilian Amazon declined by 70% between 2004 and 2014 (*7*), avoiding the equivalent of 12% of global annual CO_2 emissions (*8*), the main *GHG* causing climate change. Yet, emissions of CO_2 and other *GHG*s (e.g., CO, CH_4, NOx, N_2O) associated with wildfires accelerated during this period. Interactions between agricultural activities, illegal fires, and extreme weather events intensified Amazon fire regimes and their associated emissions (*9*, *10*). During the 2000s alone, ~85,000 km^2 of primary forests burned in Amazonia, mostly during the 2005 and 2010 droughts linked to the warm phase of the Atlantic Multidecadal Oscillation (*AMO*) (*9*). In 2015, the central Amazon experienced a similar spike in fire activity during another severe and widespread drought event, triggered by anomalous warming of both the tropical Pacific (*El Niño*) and the tropical North Atlantic(*9*). Superimposed upon these episodic droughts, climate change is expected to promote even more frequent, intense and extensive drought events. The strong climatic control over these wildfire events (*11*) suggests that forest flammability will increase in the near future even if deforestation rates decline (*5*). Addressing large-scale forest degradation by Amazon wildfires is therefore critical to quantifying future global C emissions.

In Amazonia, surface forest wildfires emit *GHGs* to the atmosphere via three main mechanisms. First, the combustion of fuels (e.g., leaves, twigs, and branches) instantly transfer CO_2 to the atmosphere, with most tropical wildfires contributing between 20 and 60 MgC ha^{-1} to the atmosphere (*12-14*). Second, thermal degradation of biomass causes the release of several types of *GHGs* other than CO_2, including methane (CH_4), nitrous oxide (N_2O), carbon monoxide (CO), and nitrogen oxides (NOx). Finally, post-fire tree mortality contributes CO_2 emissions to the atmosphere for several years or decades as trees decompose (*12*, *13*). Although forest recovery can partially or fully offset post-fire emissions associated with tree mortality, post-fire recovery may be slowed when high-intensity fires deplete soil nutrients, kill seeds and belowground bud (resprout) banks, and create niche spaces for invasive species such as grasses (*14*).

Here we used a coupled fire-ecosystem model (**Fig. S1**) to assess the synergies between climate change and deforestation for burned area (*BA*) and emissions of CO_2, CO, CH_4, N_2O, and NO_x (hereafter referred to as eCO_2) from forest fires across the seasonally driest portion of the Amazon. This region represents 61% of the Brazilian Legal Amazon (**Fig. 1**) and is a hotspot of forest fire activity (*10*). Our fire model simulates daily fire ignition and spread as a function of climatic conditions, land use, fuel loads, and terrain at 500-m resolution. Our ecosystem model also represents forest C dynamics and drought-induced changes in fuel loads and drying – a process that is absent in most ecosystem models (**Fig. S1**). We used this coupled model to test the hypothesis that future forest fires will be highest where (1) forest edges are most exposed to ignition sources due to deforestation and fragmentation and (2) climate becomes drier and hotter due to the

accumulation of atmospheric *GHGs*. Conversely, we expect that *BA* will decrease where high deforestation reduces fuel continuity, and where dense primary forests create a moist understory microclimate. The latter includes the interior of protected areas and indigenous reserves, referred to here as protected forests. Our model simulations from 2000 to 2050 represent two scenarios of climate change (low emissions: *RCP2.6*; high emissions: *RCP8.5*); two scenarios of deforestation (following recent trends (*D*) and no deforestation (*N*)); and, their combination (*RCP2.6D*, *RCP 8.5D*, *RCP2.6N*, *RCP 8.5N*).

Results

Model robustness

Our probabilistic fire model captured broad spatial and temporal patterns of sources of ignition and *BA* for the southern Brazilian Amazon (**Fig. 1**). The simulated number of hot pixels (our proxy for fire ignitions) was highest during the dry season and lowest during the wet season (**Fig. 2**), when low vapor pressure deficit (*VPD*) usually damps forest flammability to zero (*16*). The simulated number of hot pixels approximated observed patterns (R^2: 0.83; slope: 1.60; RMSE: 2431.88; **Fig. 2**), although there were fewer simulated ignition sources than observed. However, the subsequent simulated regional and temporal patterns of fire scars agreed with observations (R^2: 0.88; slope: 0.88; RMSE: 0.18) (**Fig. 2**). Specifically, the *BA* peaked during dry and hot years and occurred mostly along forest edges across the Arc of Deforestation, consistent with *BA* patterns typical of the southern Amazon in recent decades (*10*, *11*).

In addition to capturing spatial and temporal patterns of *BA*, our modeling framework properly represented observed patterns of fire intensity and fire severity in southern Amazonia. Once a given forested pixel ignited, our ecosystem model simulated the fireline intensity from fuel consumption (*W*), fire spread rate (*FSR*), and the constant heat yield per unit of fuel combusted. Compared with observed values from a large-scale fire experiment in southeast Amazonia (*14*), the modeled fireline intensity and associated variables (*W* and *FSR)* performed relatively well during both drought and non-drought years (**Fig. 3**). Fire intensity during the droughts of 2007 and 2010 was substantially higher than non-drought years because of the simulated variability in understory *VPD* and fuel availability. However, our model overestimated fire spread rate by 48%; underestimated fuel consumption by 25% during non-drought years; and overestimated fuel consumption by 18% during drought years.

Our coupled fire-ecosystem model was most sensitive to variability in understory *VPD*, with drought (as represented by the maximum climatological water deficit, *MCWD*) having an important secondary effect (**Fig. S2**). Thus, *BA* and eCO_2 emissions from wildfires occurred mostly during drought years that caused canopy opening and increased understory *VPD*.

Fire regimes in a changing climate – no new deforestation

Even with no new future deforestation, simulated fire regimes intensified across the southeast Amazon under climate change scenarios *RCP8.5N* and *RCP2.6N*. Compared to the 2000s, simulated forest fires in subsequent decades burned larger areas, combusted more fuels, released more energy, and emitted more eCO_2 to the atmosphere (**Fig. 4**). The gross emissions of eCO_2 resulting from these fires totalized 13.7 Pg (*RCP 2.6N*) and 16.4 Pg (*RCP8.5N*) by 2050. In general, the *RCP8.5N* scenario resulted in more severe fires but reduced burned area, compared to the conservative *GHG* emission scenario (*RCP2.6N*). As a result, we project slightly higher gross *GHG* emissions in *RCP2.6N* than in the *RCP.8.5N*. However, later in our simulation (e.g., 2040 and 2050), *BA* and eCO_2 increased more in *RCP.8.5N* than in *RCP2.6N*, suggesting that radiative forcing associated with *GHGs* is increasing forest flammability (**Table S1**). For instance, under

scenarios *RCP8.5N* and *RCP2.6N* both *BA* (39% and 31%, respectively) and fire-induced eCO_2 emissions (57% and 46%, respectively) increased in the 2050s compared to the 2000s.

Fire regimes in a changing climate – BAU deforestation

When we accounted for new deforestation in our simulations, *BA* and fire-related eCO_2 emissions increased under both climate scenarios (*RCP8.5D* and *RCP2.6D*), compared to the no deforestation simulations (*RCP8.5N* and *RCP2.6N*). Under *RCP8.5D*, simulated *BA* and gross eCO_2 emissions from forest fires between 2010 and 2050 totaled 18.6 Mha and 17.0 Pg, respectively. These values were 30% and 22% higher than in *RCP8.5N* (**Fig. 4**), suggesting strong interactions between climate change and deforestation in the near future. Overall, the scenario representing deforestation and high radiative forcing (*RCP8.5D)* yielded the highest gross eCO_2 emissions from wildfires. In contrast, the scenarios without new deforestation yielded the lowest fire-related eCO_2 emissions (**Tables S1 & S2**).

As deforestation interacted with climate change in our simulations, the number and geography of Amazon wildfires changed compared to current *BA* (**Fig. 5**). A 5% decline in forest area from 2010-2050 (due to deforestation) increased the simulated *BA* by 47% (*RCP 8.5D*) and 40% (*RCP 2.6D*) (**Fig. 4**). In the scenario representing business-a-usual deforestation rates, drought-induced fuel accumulation and drying also increased wildfire activity, even in areas experiencing low deforestation. Although protected areas and indigenous lands effectively deterred most deforestation, these forests experienced an actual increase in *BA* in the future (from 27% to 42%) due to the combined effects of high fuel loads, increased dryness, and fuel continuity. In older frontiers with more fragmented forests, the projected *BA* decreases (from -73% to -58%), probably because of the lack of large forest blocks available to burn.

Post-fire recovery – net emissions

Most fire-related *GHG* emissions in our simulations resulted from combustion and post-fire tree mortality releasing CO_2 to the atmosphere. CO_2 and CO accounted for 70% and 7% of total emissions, respectively. Together, other *GHGs* contributed 23% (Table S1). Although we expected post-fire forest regrowth to partially offset CO_2 emissions, our simulations show lower capacity of forests to recover their carbon (C) stocks in the near future. Future dry-warm climatic conditions caused reduced C stocks due to high-severity fires and larger *BA*. Post-fire recovery of C stocks also decreased because future climate conditions reduce potential forest biomass. As a result, we project that a greater proportion of C emissions from future forest fires will remain in the atmosphere, rather than being assimilated back into forests. Assuming average rates of biomass recovery, cumulative net C emissions (emissions minus recovery) from these fires could reach 1 PgC for both *RCP2.6N* and *RCP8.5D* scenarios between 2010 and 2050. However, our simulations show that avoiding new deforestation could reduce net emissions by 38% (*RCP2.6*) and 56% (*RCP8.5D*). Avoiding repeated burning could promote faster forest recovery of carbon stocks, given that 26% of the study region experienced repeated burning.

Discussion

In southern Amazonia, forest fire regimes have drastically changed over the past three decades (*9-11*). Interactions among human activities and extreme weather events have triggered wildfires that burn larger areas and emit more carbon to the atmosphere, even in areas where deforestation has declined (*9*). During the early 21st Century, some studies estimated that escaped forest fires accounted for a third of total emissions from deforestation, with emissions from wildfires likely surpassing those from deforestation in extreme drought years (*9*). Our projections support these previous findings and point to an acceleration of fire activity in southern Amazonia in the coming decades. As the climate becomes drier and hotter, our projections suggest that 16% of the region's forests will burning the next few decades. The eCO_2 emissions from these fires could reach 6.0 Pg

in the 2050s, compared with 2.1 Pg in the 2000s. If deforestation continues at current (relatively low) levels, emissions from forest fires will regularly surpass those from deforestation. Decreasing global *GHG* emissions to near zero may reduce the likelihood of severe droughts and associated wildfires, but mostly after 2040. The climate changes already committed for the region will thus increase wildfire activity over the short term, supporting a body of studies projecting an intensification of forest fire regimes in Amazonia (*5*, *17*).

Despite the likely intensification of fire regimes in southern Amazonia, deterring new deforestation could substantially reduce *BA* and associated emissions. Compared with the (BAU) deforestation scenarios, we project that preventing new Amazon deforestation reduced *BA* and eCO_2 emissions by up to 30% and 50%, respectively. With no deforestation, the perimeter of forests exposed to sources of ignition is expected to decrease, leading to lower *BA* (*18*). However, we observed a nonlinear relationship between forest fragmentation and *BA*. Across highly fragmented regions, for instance, *BA* was limited by the lack of fuels. In contrast, large tracts of primary forests became flammable and experienced increased burning, but only when dry-warm climatic conditions drove forest thinning and associated increases in understory dryness after 2030. Primary forests in southern Amazonia were less likely to burn early in our simulations due to their high canopy cover and associated fuel moisture, but they became flammable as droughts and high atmospheric VPD increased fuel availability by warming the forest understory and increasing fuel loads. There is ample empirical evidence supporting these behaviors in our model, given that soil drying tends to cause increased mortality of large trees and associated fuel availability (*19-22*).

As large tracts of primary forests become flammable, our model projects more protected forests to burn in the coming decades. Although protected forests have effectively deterred most deforestation and promoted high fuel continuity, the moist forest understory inside those areas prevent fires from spreading in most years. However, fuel moisture began to increase in our simulations over time, because droughts became more intense and frequency and background vapor pressure deficit increased. Consequently, fires in the future burned larger areas inside protected forests. Our results suggest that preventing such increases in fire activity may require a large effort to lower sources of ignition.

In agreement with recent observations (*15*), droughts controlled most of the spatial-temporal patterns in *BA* and fire-induced emissions in our simulations, with projected regional warming playing an important secondary role. Two major assumptions allowed our fire-ecosystem model to represent such patterns. First, drought-induced fuel accumulation and drying in our model changed as in 2005, when a severe drought caused increased mortality of Amazonian trees (*23*). While this assumption is likely to hold in the near future, modeling drought-induced changes in forest disturbance and fuel dynamics under extreme climate change into the distant future would require explicit representation of physiological processes, such as plant hydraulic failure, drought-induced C starvation (*24*), and changes in forest resilience due to CO_2 fertilization (*2*). To date, the development and application of such models for tropical systems have been hampered by our poor understanding of how extended dry periods affect canopy phenology and tree mortality (*25*). Our simulations also lack several stressors that could slow biomass accumulation even further (e.g., liana infestation, nutrient depletion, and windthrow events, among others(*26*)).

Despite the complex processes affecting fire behavior, intensity, and severity in tropical forests, our modeling approach captured major features of forest fire behavior and severity for southern Amazonia. However, we assume that drought frequency during the 2000s is representative of future drought regimes, while drought intensity and extent will change with future climate projections. This implicitly assumes that the *AMO* will remain in a warm phase in the coming decades and that

drought extents will be similar to those during the 2000s. This characteristic of our model probably underestimated *BA* and fire-induced C emissions in the central and eastern Amazon—where extended dry periods are also triggered by ENSOs. Advances in climate projections are needed to better represent the teleconnections among future greenhouse gas emissions, changes in sea surface temperature anomalies, and Amazon precipitation patterns.

The projected intensification of Amazon fire regimes under both *RCP2.6* and *RCP8.5* climate scenarios underscores the need to counteract increasing fire risk and conserve Amazon forests. Avoiding deforestation could substantially reduce fire-induced C emissions (e.g., up to 50% in our simulations), but not enough to offset increases associated with climate change. A transition away from fire-dependent to fire-free agricultural and agroforestry systems would reduce sources of ignition and ultimately wildfires (*22*), a trend that has already been observed in some tropical regions (*28*). Where there is a strong socioeconomic dependence on slash-and-burn systems, fire management techniques should be employed to minimize the risk of agricultural fires escaping into neighboring forests. Command-and-control operations against illegal agricultural fires are another important tool to prevent wildfires (*22*). Furthermore, expanding the existing network of well-trained and equipped fire brigades could enhance Brazil's ability to suppress unwanted fires. Finally, specialized weather forecast systems and fire behavior models have effectively guided fire suppression efforts in many countries, often months before the fire season starts (*29*). These strategies could be readily adapted to and implemented in Brazil (*30*).

Aggressive efforts to reduce sources of fire ignition and suppress unwanted fires could significantly reduce the likelihood of burning large tracts of Amazonian forests, including protected areas and indigenous reserves. These actions will be most effective if accompanied by a global decrease in greenhouse gas concentrations in the atmosphere. Particularly after 2040, increased *GHG* emissions may create much more flammable landscapes by triggering widespread droughts and regional warming in Amazonia (*5*). In the absence of sharp reductions in global *GHGs* to mitigate these negative effects, local and regional efforts to reduce fire probability may yield only short-term results.

Materials and Methods

Study area

The study area comprises the meridional Brazilian Amazon, where prolonged dry seasons (3-5 months with precipitation ≤ 100 mm) create conditions for understory forest fires, especially during drought years. The total modelled area is ~192 Mha, of which 72% is covered by native forests. The main land use in deforested areas is cattle ranching, with mechanized agriculture ranking second (*31*).

Modeling

To address the question of how climate and land-use change may affect fire regimes in Amazonia, we used a coupled fire-ecosystem model(*32*, *33*). Our fire model (fire ignition and spread for carbon, FISC; **Fig. S1**) simulates monthly fire ignition and *BA* at a resolution of 25 ha for the Amazon region (*32*, *34*), while our ecosystem model (carbon and land use; CARLUC) simulates monthly forest carbon dynamics as a function of climatic variables (*17*). Below we describe each component of the models used in this study.

Fire ignition.

FISC estimates the likelihood of agricultural fires igniting a wildfire by combining two probabilities. First is the climatic probability of fire ignition, estimated from monthly maps of climate dryness (e.g., Vapor Pressure Deficit, VPD) from the Climate Research Unit (CRU) and NCEP/NCAR databases (**Table S3**). Second is the probability of active fires ("hot-pixels") occurring in deforested fields near forest edges (≤ 4 km), estimated annually based on a set of biophysical spatial variables—including location and size of urban areas and deforestation (**Table S3**). Once these probabilities are calculated, FISC evaluates whether their sum exceeds a random number generated according to a beta distribution (*32*). If this random number is exceeded, FISC simulates a successful source ignition (**Fig. S1**) (*1*). This model has been extensively calibrated and validated for the Amazon using active fire data (*34*).

Fire spread

FISC simulates fire propagation using cellular automata (CA). Specifically, if a given forested cell is ignited by an agricultural fire, FISC calculates the probability of this ignition source spreading into each neighboring cell for each model iteration (i.e., 30 per month) (**Fig. S1**). There are five sets of variables defining whether fire spread will occur (**Table S4**): wind intensity and direction (*32*); fine fuel loads estimated by our ecosystem model (CARLUC); terrain features such as upslope direction, obstacles, and different land uses (*32*, *34*); and microclimate conditions (i.e., forest understory VPD) estimated by CARLUC. The fire spread module has been calibrated and validated using fire scar maps from Morton et al. (*10*). Our results show that FISC captured the spatial-temporal variability in fire scars across the southern Amazon during the 2000s (**Fig. 3**).

Ecosystem model

CARLUC (Carbon and Land Use Change) is a process-based carbon cycle model that borrows its basic structure from the Physiological Processes Predicting Growth (3 PG) forest model (*35*). CARLUC estimates net primary productivity (NPP) from plant available water (PAW), photosynthetically active radiation (PAR), VPD, and air temperature (**Table S5**). During each

monthly time step, NPP is allocated to wood, leaf, and root carbon pools. Mortality creates necromass that is placed in structural leaf litter, metabolic leaf litter, structural root litter, metabolic root litter, coarse woody debris and humus pools. Leaf litter and small woody fuels (i.e., 1-h fuels) are considered as the fuel load (*17*). In addition to carbon dynamics, CARLUC simulates (a) drought-induced effects on fuel dynamics; (b) litter moisture content (LMC, %), estimated from VPD; (c) fire spread rate (FSR, $m \cdot min^{-1}$), estimated from LMC; (d) fire fuel consumption (W, $kg \cdot m^{-1}$), estimated from LMC and fuel load mass; (e) fire line intensity (FI, $kW \cdot m^{-1}$), estimated from FSR and W; and (f) fire-induced biomass losses, derived from field measurements of FI (*17*).

CARLUC's representation of the relationship between drought and changes in biomass was derived from the Amazon forest inventory network (*23*). Specifically, changes in aboveground biomass and the maximum climatological water deficit (ΔMCWD) observed during the 2005 drought were compared with the long-term average. CARLUC assumes that when ΔMCWD drops below -40 mm, CARLUC simulates losses in aboveground biomass following a linear function of ΔMCWD (*36*). This process triggers associated changes in fuel loads and moisture. The fire model has been calibrated for the southern Amazon using data from a large-scale fire experiment (*15*).

Once a given pixel of forest burned in our simulations, emissions of greenhouse gas emissions were estimated for CO_2, CO, CH_4, N_2O, and NO_x. We assumed that fuel consumption of necromass generated emissions of CO_2, CO, CH_4, N_2O, and NO_x, following emission factors from IPCC (*37*).

Climate projections

Our fire and ecosystem models were forced with climate data representing two levels of future global radiative forcing, the representative concentration pathway (RCP) 2.6 Wm^{-2} and 8.5 Wm^{-2}. *RCP2.6* assumes negative emissions and is the scenario most closely mirroring the Paris (COP21) agreement. *RCP8.5* represents "business-as-usual" fossil fuel emissions (*38*). To run our fire-ecosystem model, we used simulations from the three climate models participating in the Coupled Model Intercomparison Project Phase 5 (CMIP5) that best represent historical temperature patterns and precipitation seasonality for the Amazon: Hadgem2-es (*39*), Miroc-esm (*40*), and Mri-cgcm3 (*40*) (**Fig. S2**). We used temperature data from CRU and precipitation from the Tropical Rainfall Measuring Mission (TRMM; 3B42 product) to evaluate and bias-correct these climatic variables.

To estimate potential changes in VPD in the coming decades, we assumed that future changes in air temperature would drive changes in VPD by correcting the mismatch between modeled and observed climate. Specifically, we sliced projected air temperature time-series into historical (1950-2005) and future (2006-2050) periods. Next, we estimated the rate of change of temperature (ΔT) between historical and future projections. We then modeled the saturation pressure as a function of ΔT (**eq. 1**), adding this change in saturation pressure (Δes) to the observed saturation pressure (**eq. 2**). Observed saturation pressure and relativity humidity were cycled over the 2000s period.

eq. 1: $$\Delta es\ (T) = 0.611\, exp\left(\frac{17.21\Delta T}{\Delta T + 237.3}\right)$$

eq. 2: $$VPD\ (es, rh) = \left(1 - \frac{rhmax}{100}\right)\ (\ es + \ \Delta es)$$

Because the variability in precipitation projected by our climate models was substantially lower than the observed data (*42*), we applied the climate variability from the 2000s to future projections,

adding it to the projected changes in precipitation. With this approach, the spatial patterns of drought are constrained mostly to the regions that experienced unusually low precipitation during the 2000s, a decade dominated by drought events associated with the warming phase of the Atlantic Multidecadal Oscillation (*AMO*). This prescribed future climate was then used to calculate the MCWD within each decade (*43*).

Deforestation projections

OTIMIZAGRO is a spatially explicit model that simulates land use, land-use change, forestry, deforestation, and regrowth under various scenarios of agricultural land demand and deforestation policies for Brazil (*44*). The model simulates nine annual crops (including single and double cropping); five perennial crops, and plantation forests. The model framework, developed using the Dinamica EGO platform (*45*), is structured in four spatial levels: (i) Brazil's biomes, (ii) IBGE micro-regions, (iii) Brazilian municipalities, and (iv) a raster grid of 25 ha spatial resolution. Future demand for crops, deforestation, and regrowth rates are exogenous to the model. Projected annual deforestation rates (3,100 $km^2\ yr^{-1}$) (**Fig. S3**) consist of 2009-2014 averages for southern Amazonia (INPE 2015) (*7*). The spatial distribution of deforestation is a function of spatial determinants, such as distances to roads and previously deforested areas.

Simulations

To simulate potential changes in Amazon fire regimes, we performed four numerical experiments based on future climate and deforestation scenarios. In these experiments, we compared climate and deforestation impacts on fire regimes as a function of two different levels of global warming at the mid-century (2050), the *RCP 2.6* and *RCP 8.5* scenarios, and two scenarios of deforestation (no deforestation and deforestation following historical trends).

Acknowledgments

General: We thank R. Houghton, B. Rogers, P. Duffy, and L. Rattis for helpful suggestions on the manuscript.

Funding: P.M.B and B.S.F received funding from the World Bank. P.M.B was supported by NSF (DEB #1457602), NASA (IDS # NNX14AD29), the Gordon and Betty Moore Foundation (grant GBMF #5483), and NORAD.

Author contributions: B.S.F, L.R, A.A, and P.M.B. designed the model and conducted data analyses. P.M.B. wrote the manuscript with input from all authors. B.S.F, E.C.M.F, and P.M.B. conceived the study.

Competing interests: The authors declare no competing financial interests.

Data and materials availability: Model simulation output is archived with the supporting information, and full data sets are available on request.

Figures and Tables

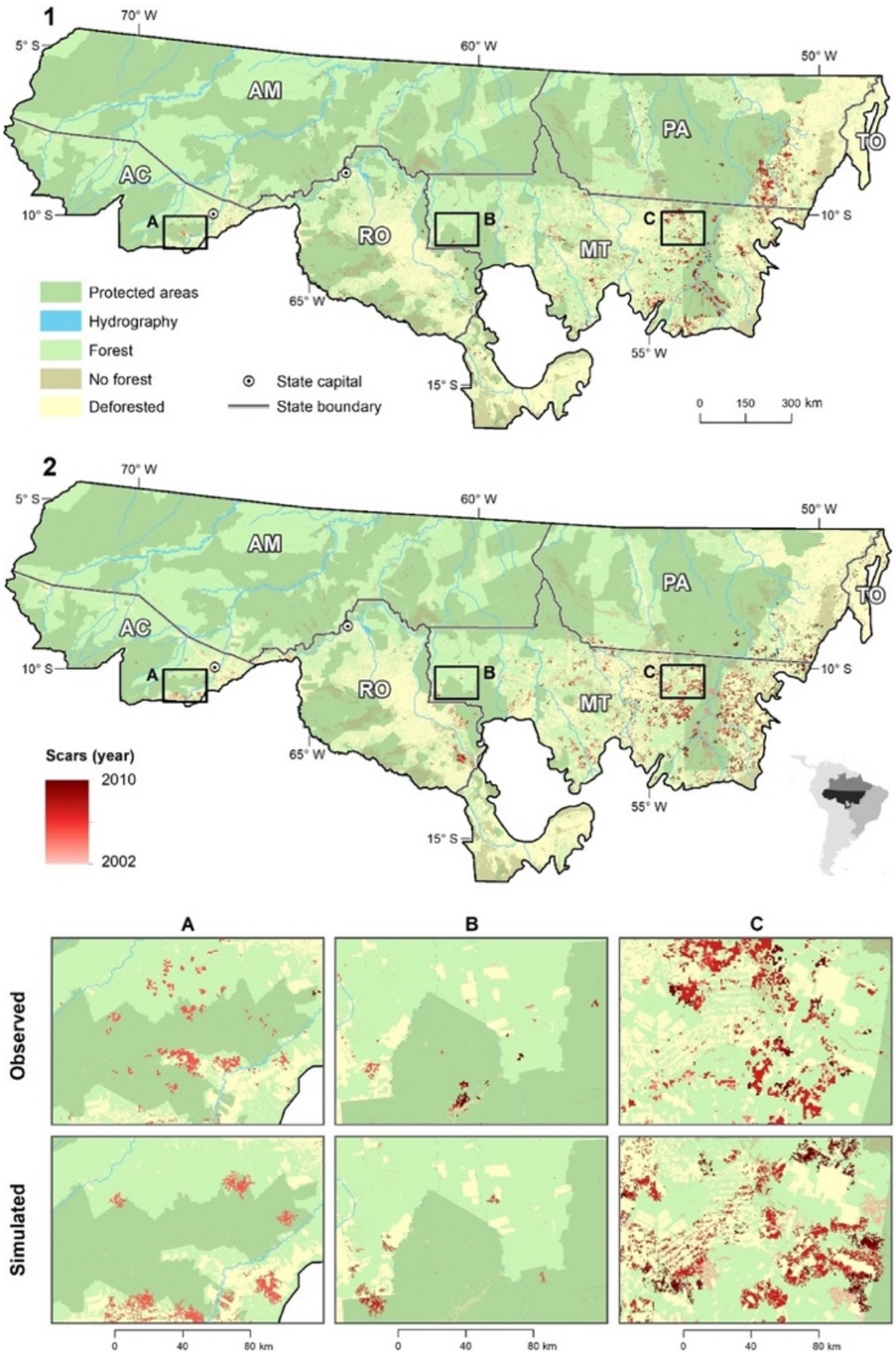


Fig. 1. Historical patterns of burned area across Brazil's southern Amazon for the period 2002-2010. Panel 1 (*Top*): Observed fire scars from Morton et al. (*10*). Panel 2 (*Middle*): Simulated fire scars based on our fire model (FISC). Panel 3 (*Bottom*): Observed (upper panel) and simulated (lower panel) patterns of burned area for three regions of the southern Amazon (indicated on the upper panels).



Fig. 2. Seasonal patterns of active fires in deforested areas near forest edges (≤ 4 km) for the southern Amazon. Panel A - Seasonal patterns in active fires ("hot Pixels") in deforested areas near forest edges (≤ 4 km) for the southern Amazon in 2003. "Observed" stands for NOAA – 12 satellite night active fires (*10*), while "Simulated" FISC active fires. The correlation between observed and simulated active fires was strong ($r^2 = 0.91$) and significant ($p < 0.01$). **Panel B - Annual variability in burned area (BA; understory fires) for the southern Amazon using a coupled fire-ecosystem model**. The correlation between observed ((*10*) and simulated active fires was strong (r2 = 0.94) and significant ($p < 0.01$).

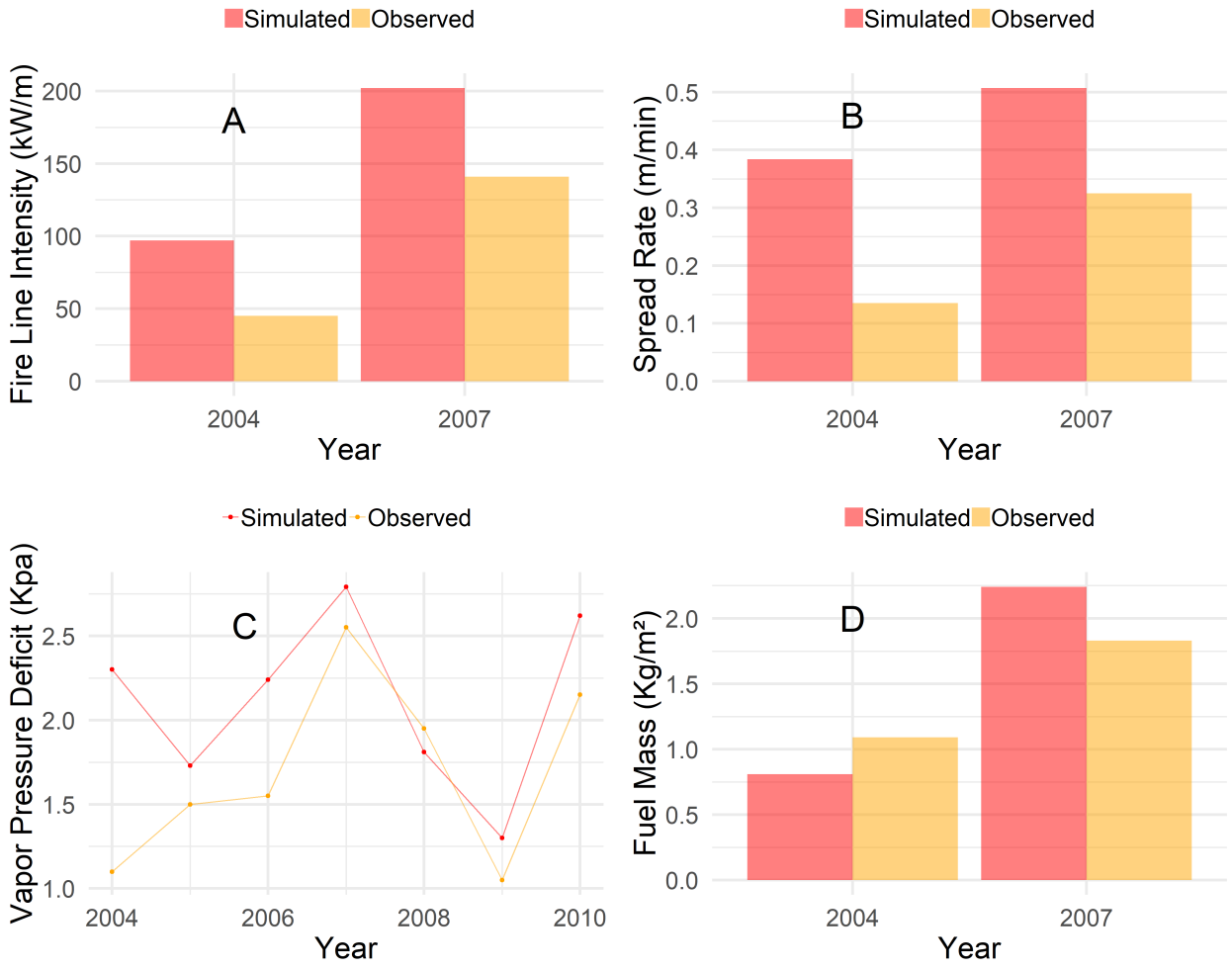


Fig. 3. Simulated and observed patterns in fire behavior for southeast Amazonia. Observed data were collected in the context of a large-scale fire experiment, in which 50-ha experimental plots were burned annually (with exception of 2008) or triennially between 2004 and 2010 (6). During 2007 and 2010, the region experienced severe droughts and increased air temperature. (A) fireline intensity. (B) rate of fire spread. (C) understory vapor pressure deficit (VPD). (C) fuel mass consumed by the experimental fires.

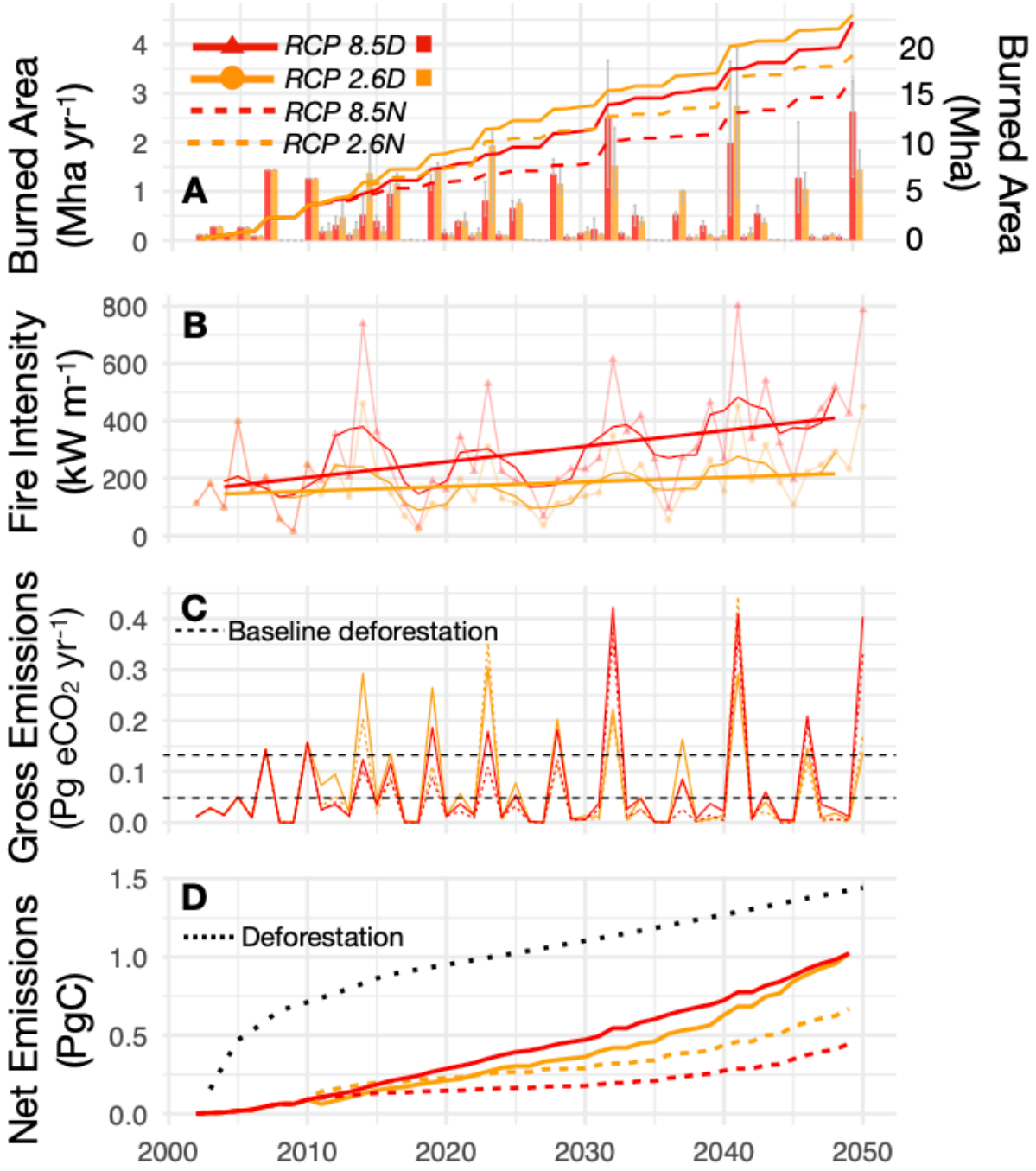


Fig. 4. Fire regime metrics for the southern Brazilian Amazon between 2001 and 2050. Panel A: Annual burned area (first y-axis; bars) and cumulative burned area (second y-axis; lines) projected under two climate change scenarios (RCP 2.6 and RCP 2.6; solid lines) and two deforestation scenarios (D: business-as-usual; N: no new deforestation; dashed lines). The bars represent only the RCP8.5D and RCP2.6D scenarios. Panel B: fire intensity, represented by 5-year moving averages (solid lines) and annual values. Panel C: annual gross carbon emissions from projected wildfires. Dashed lines represent deforestation baselines for the periods 2000-2005 (upper line) and 2006-2010 (lower line). Panel D: net emissions from modeled deforestation (dotted black line) and forest fire scenarios (colored lines).

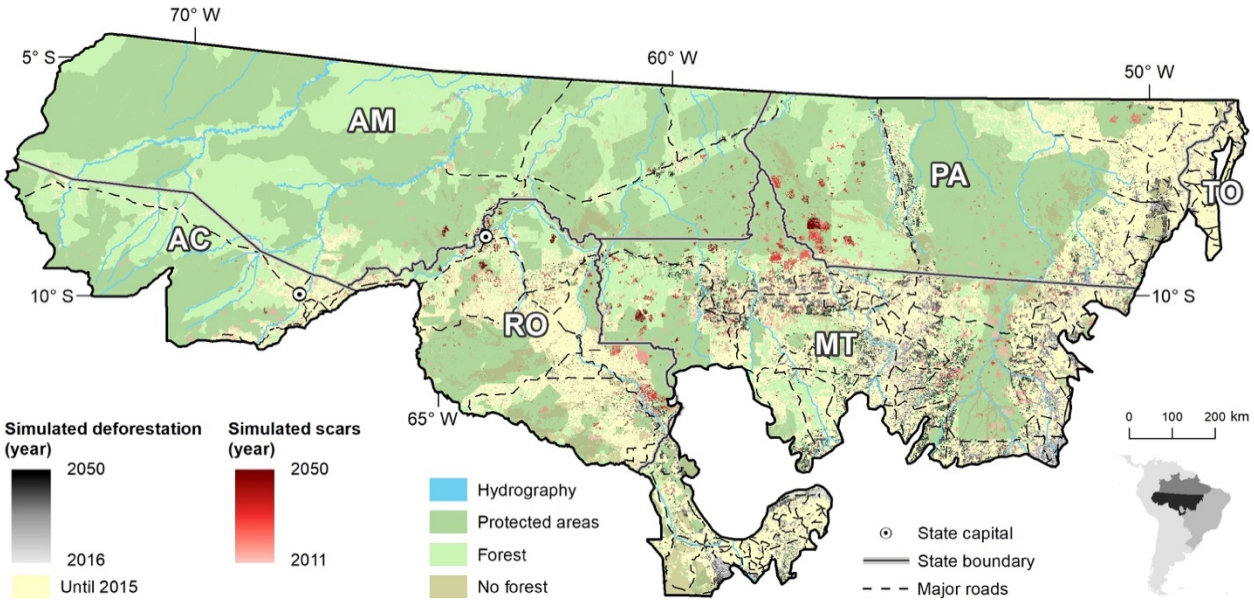


Fig. 5. Projected deforestation and burned area. Future projections of fire scars and deforestation for Brazil's southern Amazon from 2011 and 2050 under the *RCP8.5D* scenario. Darker green represents protected areas and indigenous reserves, while yellow colors show deforested areas.

References and Notes

1. C. A. Nobre *et al.*, Land-use and climate change risks in the Amazon and the need of a novel sustainable development paradigm. *Proceedings of the National Academy of Sciences of the United States of America*. **113**, 10759–10768 (2016).
2. A. Rammig *et al.*, Estimating the risk of Amazonian forest dieback. *New Phytologist*. **187**, 694–706 (2010).
3. J. K. Balch *et al.*, The Susceptibility of Southeastern Amazon Forests to Fire: Insights from a Large-Scale Burn Experiment. *BioScience*. **65**, 893–905 (2015).
4. P. M. Brando *et al.*, Abrupt increases in Amazonian tree mortality due to drought-fire interactions. *Proceedings of the National Academy of Sciences*. **111**, 6347–6352 (2014).
5. Y. Le Page *et al.*, Synergy between land use and climate change increases future fire risk in Amazon forests. *Earth Syst. Dynam.* **8**, 1237–1246 (2017).
6. D. C. Nepstad, C. M. Stickler, B. S. Filho, F. Merry, Interactions among Amazon land use, forests and climate: prospects for a near-term forest tipping point. *Philos. Trans. R. Soc. Lond., B, Biol. Sci.* **363**, 1737–1746 (2008).
7. D. Nepstad *et al.*, Slowing Amazon deforestation through public policy and interventions in beef and soy supply chains. *Science*. **344**, 1118–1123 (2014).
8. C. Le Quéré *et al.*, Global Carbon Budget 2016. *Earth Syst. Sci. Data*. **8**, 605–649 (2016).
9. L. E. O. C. Aragão *et al.*, 21st Century drought-related fires counteract the decline of Amazon deforestation carbon emissions. *Nature Communications*. **9**, 1–12 (2018).
10. D. C. Morton, Y. Le Page, R. DeFries, G. J. Collatz, G. C. HURTT, Understorey fire frequency and the fate of burned forests in southern Amazonia. *Philosophical Transactions of the Royal Society B: Biological Sciences*. **368**, 20120163–20120163 (2013).
11. A. A. Alencar, P. M. Brando, G. P. Asner, F. E. Putz, Landscape fragmentation, severe drought, and the new Amazon forest fire regime. *Ecological Applications*. **25**, 1493–1505 (2015).
12. C. V. J. Silva *et al.*, Drought-induced Amazonian wildfires instigate a decadal-scale disruption of forest carbon dynamics. *Philos. Trans. R. Soc. Lond., B, Biol. Sci.* **373**, 20180043–12 (2018).
13. D. V. Silvério *et al.*, Fire, fragmentation, and windstorms: A recipe for tropical forest degradation. **44**, 7793–7712 (2018).
14. P. M. Brando *et al.*, Abrupt increases in Amazonian tree mortality due to drought–fire interactions. *Proceedings of the National Academy of Sciences of the United States of America*. **111**, 6347–6352 (2014).
15. A. A. Alencar, P. M. Brando, G. P. Asner, F. E. Putz, Landscape fragmentation, severe drought, and the new Amazon forest fire regime. *Ecological Applications*. **25**, 1493–1505 (2015).
16. D. Ray, D. Nepstad, P. Moutinho, Micrometeorological and Canopy Controls of Fire Susceptibility in a Forested Amazon Landscape. *Ecological Applications*. **15**, 1664–1678 (2005).
17. B. L. De Faria, P. M. Brando, M. M. Environmental, 2017, Current and future patterns of fire-induced forest degradation in Amazonia. *Environ. Res. Lett.*
18. A. Alencar, C. Vera, Forest Understory Fire in the Brazilian Amazon in ENSO and Non-ENSO Years : Area Burned and. *Earth Interact.* **10** (2006).
19. V. Leitold *et al.*, El Niño drought increased canopy turnover in Amazon forests. *New Phytol.* **219**, 959–971 (2018).

20. P. M. Brando *et al.*, Drought effects on litterfall, wood production and belowground carbon cycling in an Amazon forest: results of a throughfall reduction experiment. *Philos. Trans. R. Soc. Lond., B, Biol. Sci.* **363**, 1839–1848 (2008).
21. P. Meir *et al.*, The effects of drought on Amazonian rain forests. *Geophys. Monogr. Ser.* **186**, 429–449 (2009).
22. D. Nepstad, G. Carvalho, A. C. Barros, A. Alencar, Road paving, fire regime feedbacks, and the future of Amazon forests. *Forest Ecology and Management*, 395–407 (2001).
23. O. L. Phillips *et al.*, Drought sensitivity of the Amazon rainforest. *Science*. **323**, 1344–1347 (2009).
24. L. Rowland *et al.*, Death from drought in tropical forests is triggered by hydraulics not carbon starvation. *Nature*. **528**, 119–122 (2015).
25. N. McDowell *et al.*, Drivers and mechanisms of tree mortality in moist tropical forests. *New Phytologist*. **1**, 1285–20 (2018).
26. N. McDowell *et al.*, Drivers and mechanisms of tree mortality in moist tropical forests. *New Phytologist*. **1**, 1285–19 (2018).
27. C. R. Schwalm *et al.*, Global patterns of drought recovery. *Nature*. **548**, 202–205 (2017).
28. N. Andela *et al.*, A human-driven decline in global burned area. *Science*. **356**, 1356–1362 (2017).
29. T. F. Morello, L. Parry, N. Markusson, J. Barlow, Policy instruments to control Amazon fires: A simulation approach. *Ecological Economics*. **138**, 199–222 (2017).
30. Y. Chen *et al.*, Forecasting Fire Season Severity in South America Using Sea Surface Temperature Anomalies. *Science*. **334**, 787–791 (2011).
31. S. A. Spera, A. S. Cohn, L. K. VanWey, Recent cropping frequency, expansion, and abandonment in Mato Grosso, Brazil had selective land characteristics. *Environmental Research Letters*. **9**, 064010 (2014).
32. R. A. Silvestrini *et al.*, Simulating fire regimes in the Amazon in response to climate change and deforestation. *Ecological Applications*. **21**, 1573–1590 (2011).
33. A. I. Hirsch, W. S. Little, R. A. Houghton, N. A. Scott, J. D. White, The net carbon flux due to deforestation and forest re-growth in the Brazilian Amazon: analysis using a process-based model. *Global Change Biol*. **10**, 908–924 (2004).
34. B. Soares-Filho *et al.*, Forest fragmentation, climate change and understory fire regimes on the Amazonian landscapes of the Xingu headwaters. *Landscape Ecol*. **27**, 585–598 (2012).
35. J. J. Landsberg, R. H. Waring, A generalised model of forest productivity using simplified concepts of radiation-use efficiency, carbon balance and partitioning. *Forest Ecology and Management*. **95**, 209–228 (1997).
36. S. L. Lewis, P. M. Brando, O. L. Phillips, G. M. F. van der Heijden, D. Nepstad, The 2010 Amazon Drought. *Science*. **331**, 554–554 (2011).
37. IPCC—Intergovernmental Panel on Climate Change 2006 IPCC Guidelines for National Greenhouse Gas Inventories, Prepared by the National Greenhouse Gas Inventories Programme (Kanagawa: Institute for Global Environmental Strategies)
38. D. P. van Vuuren *et al.*, The representative concentration pathways: an overview. *Climatic Change*. **109**, 5–31 (2011).
39. C. D. Jones, J. K. Hughes, N. B. G. Model, 2011, The HadGEM2-ES implementation of CMIP5 centennial simulations. *search.proquest.com*
40. S. Watanabe, T. Hajima, K. S. G. Model, 2011, MIROC-ESM 2010: Model description and basic results of CMIP5-20c3m experiments.

41. S. YUKIMOTO *et al.*, A New Global Climate Model of the Meteorological Research Institute: MRI-CGCM3 —Model Description and Basic Performance—. *Journal of the Meteorological Society of Japan. Ser. II*. **90A**, 23–64 (2012).
42. P. B. Duffy, P. Brando, G. P. Asner, C. B. Field, Projections of future meteorological drought and wet periods in the Amazon. *Proceedings of the National Academy of Sciences of the United States of America*. **112**, 13172–13177 (2015).
43. L. E. O. C. Aragão *et al.*, Spatial patterns and fire response of recent Amazonian droughts. *Geophys. Res. Lett.* **34**, L07701 (2007).
44. B. Soares-Filho *et al.*, Brazil's Market for Trading Forest Certificates. *PLoS ONE*. **11**, e0152311–17 (2016).
45. B. Soares-Filho, H. Rodrigues, M. Follador, A hybrid analytical-heuristic method for calibrating land-use change models. *Environmental Modelling and Software*. **43**, 80–87 (2013).

Supplementary Materials

Fig. S1. Components of our modeling framework.
Fig. S2. Spatial-temporal changes in vapor pressure deficit (VPD) and maximum climatological water deficit (MCWD).
Fig. S3. Projected deforestation for the southern Amazon.

Table S1. Simulated fire-related Carbon Equivalent metrics per decade.
Table S2. Simulated fire regime metrics per decade.
Table S3. Input variables used to run the fire ignition component of our fire model.
Table S4. Input variables used to run the fire spread component of our fire model.
Table S5. Input variables used to run our ecosystem model.

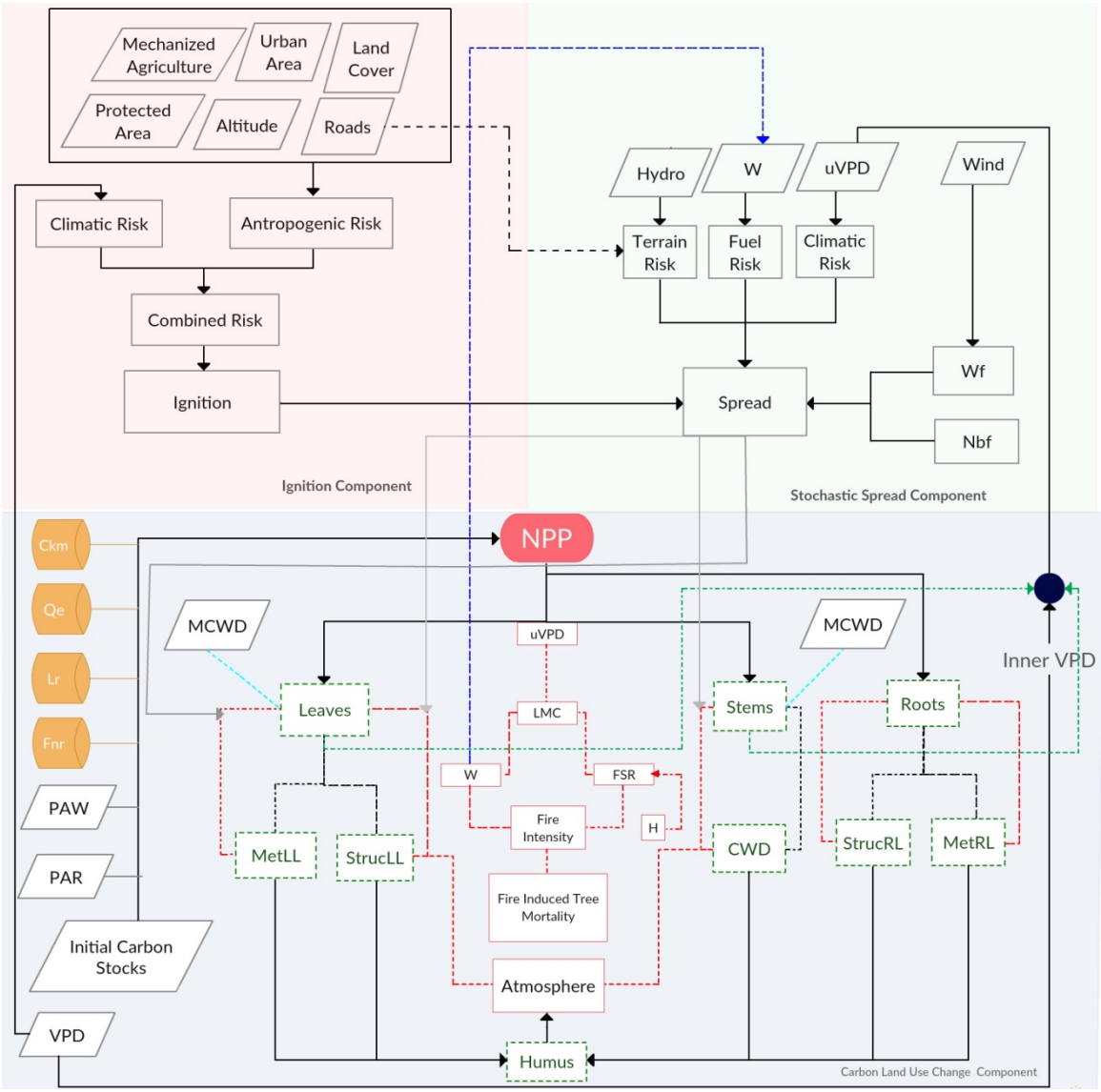


Fig. S1. Components of our modeling framework. The upper left panel shows the fire ignition module of FISC. The upper right panel shows the stochastic fire spread component of FISC. The lower panel shows the main component of our carbon model (CARLUC). The following variables are included in this diagram: ydro (hydrography); uVPD (understory Vapor Pressure Deficit); W (Fuel loads); Wf (Wind factor); Nbf (Neighboor factor); Ckm (Constant factor); Qe (Quantum Eficiency); Lr (Constant factor); NPP (Net Primary Productivity); MetLL (Metabolic Leaf Litter); StrucLL (Structural Leaf Litter); CWD (Wood Debris); StrucRL (Structural Root Litter); MetRL (Metabolic Root Litter); LMC (Litter Moisture Content); and FSR (Fire Spread Rate).

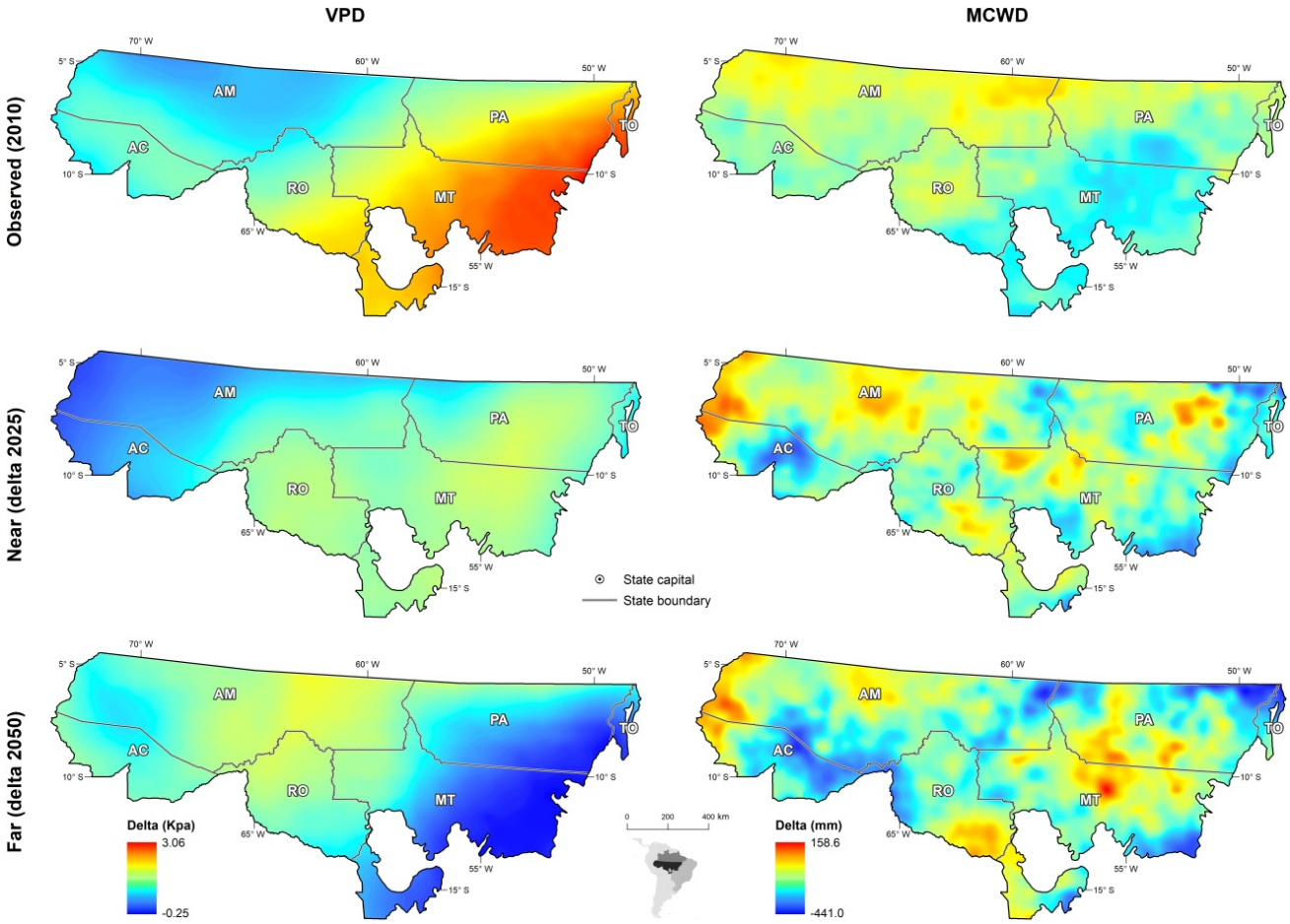


Fig. S2. Spatial-temporal changes in vapor pressure deficit (VPD) and maximum climatological water deficit (MCWD) for three time periods compared to 2010. Observed VPD and MCWD were derived from Climate Research Unit (CRU – max temperature) and TRMM precipitation datasets, respectively. Upper panel: observed climate data. Mid panel: change in VPD and MCWD between 2010 and 2025. Lower panel: change in VPD and MCWD between 2010 and 2025.

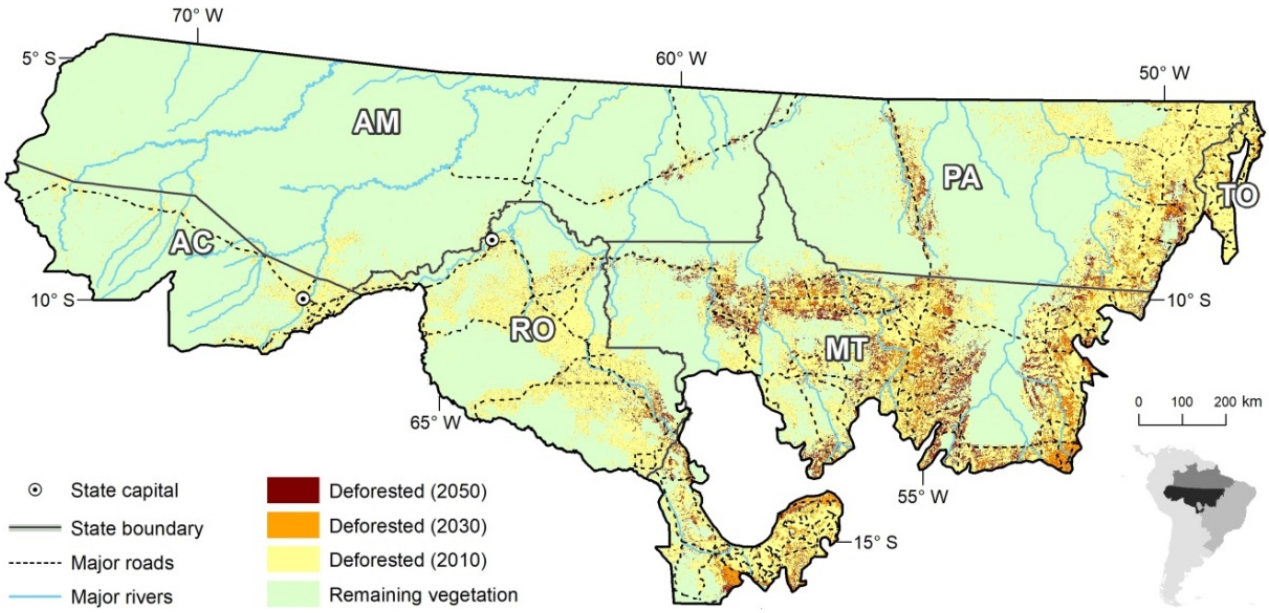


Fig. S3. Projected deforestation for the southern Amazon. Simulations were conducted based on the OTIMIZAGRO land-use model. Deforestation was binned into three time periods: up to 2010; between 2011 and 2030; and, between 2031 and 2050.

Table S1. Decadal fire related GHG emission in Carbon equivalent units (S1-A) and Burned Area (S1-B) in millions of hectares. All variables represented per Scenario.

Scenario (Decade)	CH4 (TgC)	CO (TgC)	CO2 (TgC)	N2O (TgC)	Nox (TgC)	Total (TgC)
RCP 2.6 D (2000 - 2010)	153.15	168.96	1505.62	153.05	153.07	2133.85
RCP 2.6 D (2010 - 2020)	348.40	384.37	3425.14	348.17	348.22	4854.28
RCP 2.6 D (2020 - 2030)	253.45	279.62	2491.74	253.29	253.32	3531.42
RCP 2.6 D (2030 - 2040)	176.85	195.11	1738.68	176.74	176.76	2464.15
RCP 2.6 D (2040 - 2050)	246.42	271.87	2422.63	246.26	246.30	3433.47
RCP 2.6 N (2000 - 2010)	153.15	168.96	1505.62	153.05	153.07	2133.85
RCP 2.6 N (2010 - 2020)	200.50	221.20	1971.16	200.37	200.40	2793.63
RCP 2.6 N (2020 - 2030)	216.59	238.95	2129.29	216.44	216.47	3017.75
RCP 2.6 N (2030 - 2040)	127.00	140.11	1248.54	126.91	126.93	1769.49
RCP 2.6 N (2040 - 2050)	288.48	318.27	2836.11	288.29	288.33	4019.49
RCP 8.5 D (2000 - 2010)	153.15	168.96	1505.62	153.05	153.07	2133.85
RCP 8.5 D (2010 - 2020)	202.19	223.07	1987.76	202.06	202.08	2817.15
RCP 8.5 D (2020 - 2030)	182.33	201.15	1792.50	182.21	182.23	2540.42
RCP 8.5 D (2030 - 2040)	254.49	280.77	2501.95	254.32	254.36	3545.90
RCP 8.5 D (2040 - 2050)	433.67	478.44	4263.43	433.38	433.44	6042.35
RCP 8.5 N (2000 - 2010)	153.15	168.96	1505.62	153.05	153.07	2133.85
RCP 8.5 N (2010 - 2020)	149.17	164.57	1466.51	149.07	149.09	2078.42
RCP 8.5 N (2020 - 2030)	116.96	129.04	1149.87	116.88	116.90	1629.66
RCP 8.5 N (2030 - 2040)	177.74	196.09	1747.35	177.62	177.64	2476.44
RCP 8.5 N (2040 - 2050)	359.70	396.84	3536.28	359.46	359.51	5011.80

Table S2. Burned Area (S1-B) in millions of hectares.

Decade	RCP 2.6 D (Mha)	RCP 2.6 N (Mha)	RCP 8.5 D (Mha)	RCP 8.5 N (Mha)	Total (Mha)
2000 - 2010	3.61	3.61	3.61	3.61	14.46
2010 - 2020	5.22	3.69	3.81	2.3	15.02
2020 - 2030	4.79	3.97	3.69	1.81	14.26
2030 - 2040	3.43	2.32	4.38	3.06	13.18
2040 - 2050	5.97	5.27	6.79	5.89	23.91

Table S3. Input variables used to run the fire ignition component of our fire model (FISC), the source of the data, and the link to download the data

Variable	Source	Link
Land cover	PRODES (INPE)	http://www.obt.inpe.br/OBT/assuntos/programas/amazonia/prodes
Roads	Landsat 5	http://pnlt.imagem-govfed.opendata.arcgis.com/
Urban areas	IBGE	http://downloads.ibge.gov.br/downloads_geociencias.htm
Altitude	SRTM	http://www.relevobr.cnpm.embrapa.br/download/
Mechanized agriculture	CSR/UFMG	Under Request
Vapor Pressure deficit	NCEP/NCAR	Humidity: https://www.esrl.noaa.gov/psd/data/gridded/data.ncep.reanalysis2.pressure.html Temperature: http://www.cru.uea.ac.uk/cru/data/hrg/

Table S4. Input variables used to run the fire spread component of our fire model (FISC) , the source of the data, and the link to download the data

Variable	Source	Link
Land cover	PRODES (INPE)	http://www.obt.inpe.br/OBT/assuntos/programas/amazonia/prodes
Wind	Landsat 5	https://www.esrl.noaa.gov/psd/data/gridded/data.ncep.reanalysis2.pressure.html
Hydrography	IBGE	http://downloads.ibge.gov.br/downloads_geociencias.htm
Terrain	SRTM	http://www.relevobr.cnpm.embrapa.br/download/
uVPD	NCEP/NCAR	https://www.esrl.noaa.gov/psd/data/gridded/data.ncep.reanalysis.html

Table S5. Input variables used to run our ecosystem model (CARLUC), the source of the data, and the link to download the data

Variable	Source	Link
PAW **(Plant Available Water)**	Under request (Calculated from precipitation data)	---
PAR **(Photosynthetic active radiation)**	GOES – 9 Satellite	https://www.esrl.noaa.gov/psd/data/gridded/data.ncep.reanalysis2.pressure.html
TEMP **(Temperature)**	NCEP/NCAR	https://www.esrl.noaa.gov/psd/data/gridded/data.ncep.reanalysis.html
PRC **(Precipitation)**	TRMM/NASA	http://mirador.gsfc.nasa.gov
VPD **(Vapor Pressure Deficit)**	NCEP/NCAR Reanalysis2 + CRU (Climate Research Unit)	https://www.esrl.noaa.gov/psd/data/gridded/data.ncep.reanalysis.html http://www.cru.uea.ac.uk/data